Geophys. J. Int. (2006) **164,** 15–24 doi: 10.1111/j.1365-246X.2005.02790.x

Counter-clockwise rotation of the eastern part of the Mongolia block: Early Cretaceous palaeomagnetic results from Bikin, Far Eastern Russia

Yo-ichiro Otofuji,[1] Daisuke Miura,[2] Koichi Takaba,[1] Kazuhiro Takemoto,[1] Kazutoshi Narumoto,[1] Haider Zaman,[1] Hiroo Inokuchi,[3] Ruslan G. Kulinich,[4,5] Petr S. Zimin[4] and Vladimir G. Sakhno[5]

[1]*Department of Earth and Planetary Sciences, Faculty of Science, Kobe University, Kobe, Japan. E-mail: otofuji@kobe-u.ac.jp*
[2]*Abiko Research Laboratory, CRIEPI,* 1646 *Abiko, Chiba, Japan*
[3]*School of Human Science and Environment, University of Hyogo, Himeji, Japan*
[4]*Russian Academy of Science, Pacific Oceanological Institute, Vladivostok, Russia*
[5]*Russian Academy of Science, Far East Geological Institute, Vladivostok, Russia*

Accepted 2005 August 15. Received 2005 May 18; in original form 2005 February 25

SUMMARY

We present palaeomagnetic results from Lower Cretaceous rocks in Bikin area of the Alchan basin (46.5°N, 134.7°E), Sikhote Alin orogenic belt, Far Eastern Russia. A high-temperature magnetization component with maximum unblocking temperatures at about 590°C was isolated from six sites of dacite welded tuffs in the Albian Alchanskaya Formation. The fold tests for these six sites are positive, suggesting that primary magnetization is preserved in the studied rocks. The tilt-corrected mean direction of $D = 309.3°$, $I = 68.7°$ ($\alpha_{95} = 10.1°$), with a corresponding palaeopole position at 57.0°N, 76.8°E ($A_{95} = 15.1°$), indicates a counter-clockwise (CCW) rotation for the studied area. CCW rotation is also indicated from west-directed declinations ($D = 249.1°$, $I = 64.1°$, $\alpha_{95} = 11.2°$) obtained from secondary magnetization of the Berriasian Kultukha Formation. Combining with the previously reported studies, the west-directed Cretaceous palaeomagnetic directions cover widely the eastern part of the Mongolia block. Comparison with 100 Ma palaeomagnetic pole for Eurasia shows that the eastern part of the Mongolia block experienced a CCW rotation of over 36° with respect to the Eurasian continent later than Late Cretaceous. This rotation is ascribed to post-Late Cretaceous extension that affected the continental basins (the Middle Amur, Sanjiang, Razdolnian, Amur-Zeya and Songliao basins) of the northeast Chinese Plain along the eastern margin of the Mongolia block. Contemporaneous with this CCW rotation, similar extension resulted in clockwise rotation of the eastern part of the North China block.

Key words: continent, Cretaceous, deformation, Mongolia block, palaeomagnetism, tectonics.

1 INTRODUCTION

The eastern part of the Asian continent was formed by sequential welding of four microcontinents during Palaeozoic and Mesozoic eras [Siberian craton, Mongolia block, North China block (NCB) and South China block (SCB); Fig. 1]. Collision between the Mongolia block and the NCB was completed by Permian time (e.g. Li 1998; Kravchinsky *et al.* 2002). Following this, an initial contact between the NCB and the SCB started by the Late Permian and subsequent suturing was completed by the end of Jurassic (Zhao & Coe 1987; Li 1998; Yokoyama *et al.* 2001). In the beginning of Early Cretaceous, the composite Mongolia block–NCB–SCB continent welded to the Siberian craton, which resulted in the closure of the Mesozoic Mongol-Okhotsk Ocean (Kravchinsky *et al.* 2002).

After amalgamation of East Asia during the Late Jurassic, Eastern Asia experienced widespread extension. This Late Mesozoic extension is characterized by the development of a Basin and Range type fault-basin system that extends northward to the Mongol-Okhotsk fold belt and southward to the NCB (Ren *et al.* 2002; Meng 2003). Early Tertiary extension is represented by a backarc opening of Japan Sea and South China Sea (Fournier *et al.* 2004). Several models have been proposed to explain the Late Mesozoic to Cenozoic extension. Extension has been ascribed to different tectonic events by different authors; that is, to subduction process in the Pacific (Northrup *et al.* 1995), lateral extrusion of East Asian terranes due to India–Asia

collision (Fournier *et al.* 2004), mass upwelling of asthenosphere (Tatsumi *et al.* 1989; Ren *et al.* 2002; Meng 2003) and eastward flow in the asthenosphere (Uyeda & Kanamori 1979; Flower *et al.* 2001). Origin of the extension in Eastern Asia is still in controversy.

Cretaceous-rifted Songliao and Sanjiang-middle Amur basins, and Miocene opened Japan Sea, are arranged from interior to the continental margin in the eastern part of the Mongolia block. These basins and their surrounding areas offer a unique chance to study this extensional and rifting mechanism of the continental basins that has been operative in the East Asia during Late Mesozoic to Cenozoic. Previously, post-Cretaceous counter-clockwise (CCW) rotation has been observed in the Sikhote Alin mountain area located on east side of the central Sikhote Alin fault (Otofuji *et al.* 2002, 2003). Here, we present new Cretaceous palaeomagnetic results from the Bikin area, located on west side of the central Sikhote Alin fault. The purpose is to investigate the Late Mesozoic extensional activities in East Asia.

2 GEOLOGIC SETTING AND SAMPLING

The Mongolia block is bounded to the north by the Mongol-Okhotsk Suture and to the south by the Xing-Meng Suture. The Precambrian Khingan-Bureya and Khankai massifs occupy the easternmost part of the Mongolia block, which in turn is flanked by the Sikhote Alin orogenic belt (Zonenshain *et al.* 1990; Natal'in 1993; Khanchuk 2001) (Fig. 2a).

This belt incorporates Jurassic to Late Cretaceous terranes with the East-Sikhote Alin volcanic belt, including Jurassic Samareka-Nadanhada-Bikin-Badzal-Taukh terranes, Early Cretaceous Zhuravlevka-Amur terrane, Early-Late Cretaceous Kizelevka-Monoma-Kema terranes and the East-Sikhote Alin volcanic belt. Several Mesozoic to Cenozoic basins are superimposed in the eastern part of the Mongolia block, namely, from west to east,

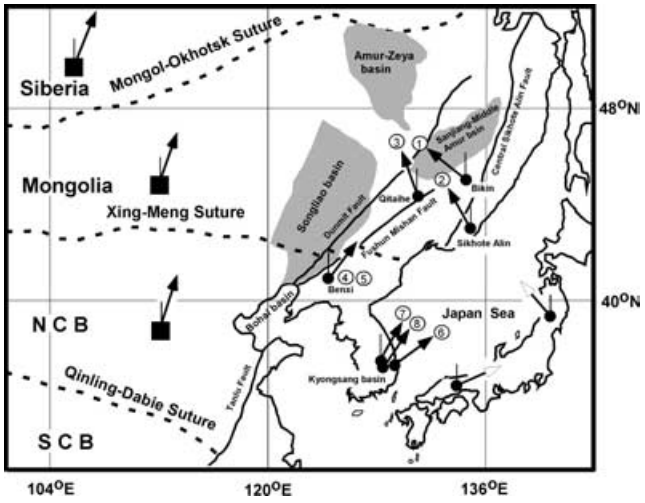

Figure 1. Simplified tectono-geographic map for the eastern margin of the Eurasian continent. Black arrows represent palaeomagnetic declinations from the Cretaceous rocks. The numbers adjacent to arrows represent the corresponding localities in Table 2. Black arrows with closed square are Cretaceous palaeomagnetic directions for Siberia (105°E, 52°N), Mongolia (112°E, 46°N) and the NCB (North China block) (112°E, 40°N), which has been calculated from the 100 Ma pole of Eurasia (Besse & Courtillot 1991). Palaeogene palaeomagnetic directions from Japanese arc rocks are shown by white arrows (Otofuji *et al.* 1985). SCB, South China block.

Songliao, Amur-Zeya, Bureya, Sanjiang-Middle Amur, Alchan, Razdolny and Partizansk basins.

The Bikin area, which forms part of the Albian-Aptian Alchan volcanic belt, is located in the Alchan basin (Fig. 2b). A neritic depositional environment was predominant during the latest Jurassic to earliest Cretaceous and the basin were buried by the Upper Jurassic–Lower Cretaceous mudstone, siltstone and conglomerate beds (Kirillova & Kiriyanova 2003). As Aptian time is characterized by volcanic activity in Southeast Russia, the sediments contained a substantial amount of volcanoclastic admixture. Abundant ammonite fauna and the Mesozoic fossil plant groups are used as markers for correlation of stage ages of the general stratigraphic scale. The Lower Cretaceous stratigraphy of the Alchan basin has been well established around the Bikin; including the Berriasian Kultukha Formation, Aptian Uktur Formation and Albian Alchanskaya Formation in ascending order.

As shown in Fig. 2(b), palaeomagnetic samples were collected at 11 sites. Although the Albian Alchanskaya Formation of the pyroclastic rocks is mapped along the Bikin river, sections suitable for palaeomagnetic investigation, that is, exposures showing consistent palaeohorizontal indicators, are few in number. A thick vegetation cover, inaccessible bank sections and avoidance from fault zones are major contributing factors. Despite these difficulties, we collected dacite welded tuffs (BK01, BK02, BK04, BK07, BK08 and BK09) and dacite tuffs (BK03) at two localities. At lower stream locality (Fig. 2b), dacite tuff (BK03) overlies (BK04, BK07, BK08 and BK09). Sandstones of the Berriaisan Kultukha Formation were collected at four sites (BK10, BK11, BK12 and BK13).

Seven to ten hand samples, oriented with magnetic compass, were collected over a distances of 20 m at each site. Accurate positioning of sites was determined by a portable navigational instrument. At all sampling sites of welded tuffs, bedding planes were observed on the basis of eutaxitic structure (lineation of stretched pumice and aligned phenocrysts). The present geomagnetic field declination value at each sampling site was evaluated from the International Geomagnetic Reference Field (Mandea & Macmillan 2000).

3 LABORATORY PROCEDURES

One to six specimens, 25 mm in diameter and about 23 mm in height, were prepared from each hand sample in the laboratory. Remanent magnetization of each specimen was measured using a 2G Enterprises cryogenic magnetometer. Stepwise thermal demagnetization was carried out up to 600° with a Natsuhara TDS-1 thermal demagnetizer; the residual field in these furnaces during the cooling cycle was less than 5 nT. A pilot specimen was selected from each site and subjected to stepwise thermal demagnetization as follows: From 100°C to 500°C at 50°C intervals, and from 530°C to 590°C at 30°C or 20°C intervals. The pyroclastic rocks of the Alchanskaya Formation show an unblocking temperature range between 560°C and 580°C. Sedimentary rocks of the Kultukha Formation are generally characterized by low unblocking temperatures below 350°C. Thus, the same demagnetization approach was adopted for the remaining specimens of the Alchanskaya Formation. For the remaining specimens of the Kultukha Formation, demagnetization step was, however, reduced to 10°C between 300°C and 350°C, and to 30°C between 350°C and 530°C.

Demagnetization response was plotted on Zijderveld diagrams (Zijderveld 1967) and equal-area projections to assess component structure and to evaluate directional stability, respectively. Principal component analysis (Kirschvink 1980) was used to determine

directional behaviour of different magnetization components. Mean directions were calculated using Fisherian statistics (Fisher 1953).

4 PALAEOMAGNETIC RESULTS

4.1 Pyroclastic rocks of the Albian Alchanskaya Formation

Dacite welded tuffs from six sites (BK01, BK02, BK04, BK07, BK08, BK09) have initial NRM intensities from 0.32×10^{-2} A m^{-1} to 95×10^{-2} A m^{-1}. Thermal demagnetization procedure generally revealed two components of magnetization (Fig. 3). A low-temperature component was unblocked between 300°C and 450°C. A high-temperature component, which shows a straightforward demagnetization behaviour, was removed between 560°C and 590°C.

Six site-mean directions with the high-temperature component reveal good clustering with precision parameter between 13.8 and 422.4 (Table 1), corresponding to small 95 per cent confidence circle ($\alpha_{95} = 2.7^\circ \sim 15.5^\circ$). These site-mean directions show two groups of declinations in geographic coordinates. Two sites from east-dipping strata (BK01, BK02) gave west-directed declinations whereas the remaining four sites from west-dipping strata revealed east-directed declinations (Fig. 4). After tilt correction, all the site-mean directions cluster in the northwest quadrant with steep inclination. The ratio of the precision parameter increases after tilt correction ($k2/k1 = 45.2/9.3$). The optimal concentration of direction-correction (DC) tilt test (Enkin 2003) is achieved at 96 ± 39 per cent, which indicates a positive tilt test. According to the McFadden (1990) method, the fold test is also positive at 99 per cent confidence level. The calculated value ($\xi 1$) is 5.3901 in geographic coordinates and 0.4376 after tilt correction, while the critical value (ξ) is 3.9190 at 99 per cent confidence level. The mean direction after 100 per cent unfolding ($D = 309.3^\circ$, $I = 68.7^\circ$, $\alpha_{95} = 10.1^\circ$, $N = 6$) is the ChRM direction of welded tuffs, which is clearly far from the present geomagnetic field direction ($D = 348.9^\circ$, $I = 62.2^\circ$).

Dacite tuffs from one site (BK03) have initial NRM intensities between 1.1×10^{-2} A m^{-1} and 2.4×10^{-2} A m^{-1}. After the unblocking of low-temperature component by 300°C, the high-temperature component with unblocking level of 590°C appeared (Fig. 3c). The site-mean direction of the high-temperature component after tilt correction ($D = 309.2^\circ$, $I = 68.5^\circ$) is parallel to the ChRM direction of the welded tuffs. However, this data is not used to calculate the mean direction of the Albian Alchanskaya Formation because of large 95 per cent confidence circle ($\alpha_{95} = 36.6^\circ$).

4.2 Sedimentary rocks of the Berriasian Kultukha Formation

Sandstones from four sites (BK10, BK11, BK12 and BK13) have initial NRM intensities between 0.14×10^{-2} A m^{-1} to $5.3 \times$

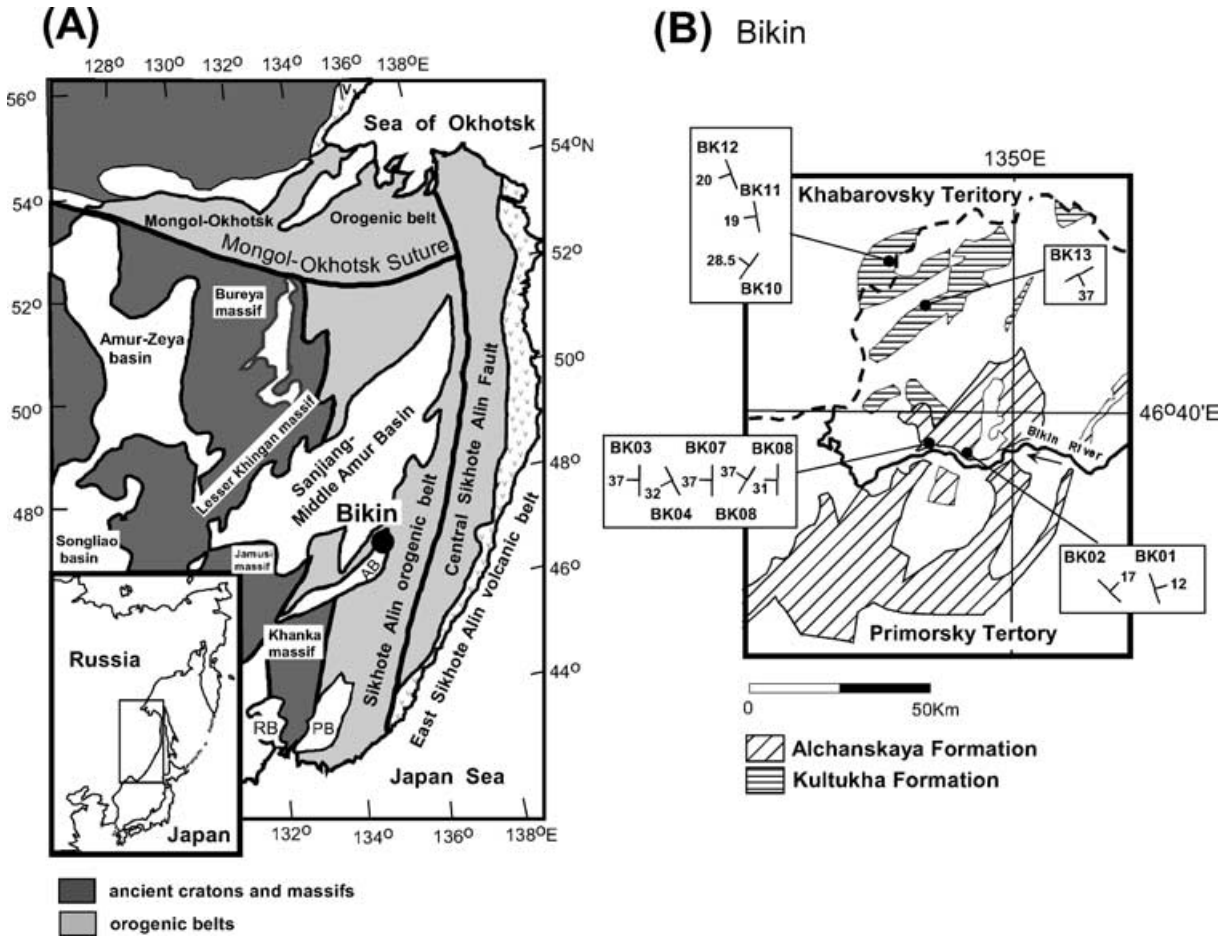

Figure 2. (a) Simplified geologic map of the study area. The shaded areas represent Cretaceous to Cenozoic basins and grabens. AB, Alchan basin; RB, Razdolny basin; PB, Partizansk basin. (b) A simplified geologic map showing the sampling localities of the Alchanskaya and Kultukha Formations in the Bikin area. Strike/dip orientations of strata are shown in insets.

Table 1. Early Cretaceous palaeomagnetic results from Bikin area of the Mongolia block.

	Locality		Strike	Dip	N/n	*In situ*		Tilt corrected				
Site No.	Lat.	Long.	(°)	(°)		Dec.(°)	Inc.(°)	Dec.(°)	Inc.(°)	κ	α_{95}(°)	Rock type
Alchanskaya Formation (Albian)												
High-temperature component												
BK03	46°33.7′	134°41.7′	181	37	8/8	43.0	62.5	309.2	68.5	3.2	36.6	Dacite tuff
BK01	46°31.8′	134°52.6	343	12	8/8	292.7	58.9	312.5	64.9	422.4	2.7	Dacite welded tuff
BK02	46°31.8′	134°52.6	315	17	7/7	82.2	53.7	311.2	55.2	124.4	5.4	Dacite welded tuff
BK04	46°33.7′	134°41.8	154	32	8/8	29.0	63.6	295.2	74.6	13.8	15.5	Dacite welded tuff
BK07	46°33.8′	134°41.9	181	37	8/8	61.8	66.2	287.2	74.1	45.3	8.3	Dacite welded tuff
BK08	46°33.7′	134°41.9	212	37	8/8	46.5	72.6	320.6	57.1	24.2	11.5	Dacite welded tuff
BK09	46°33.8′	134°42.0	182	31	8/8	70.1	61.9	319.5	84.1	17.2	13.7	Dacite welded tuff
Mean	46°.5′	134°.7′			6	8.0	76.4			9.3	23.1	Dacite welded tuff
					6			309.3	68.7	45.2	10.1	

	Pole position			
	Lat.	Long.	k	A_{95}
	57.0°N	76.8°E	24.8	12.4°

Kultukha Formation (Berriasian)												
Pyrrohotite component (100–350°C)												
BK10	47°01.4′	134°32.5	217	28.5	10/10	248.0	60.5	267.9	37.6	99.1	4.9	Sandstone
BK11	47°01.4′	134°32.5	171	19	10/10	242.9	58.8	245.1	39.9	49.5	6.9	Sandstone
BK12	47°01.5′	134°32.4	160	22	10/10	243.6	59.2	241.8	37.2	126.3	4.3	Sandstone
BK13	46°56.9′	134°39.8	64	35	9/10	272.8	76.4	165.4	62.0	164.1	4.0	Sandstone
Mean					4	249.1	64.1			68.4	11.2	
					4			240.8	49.1	8.1	34.3	
Magnetite component (350°C–580°C)												
BK13	46°56.9′	134°39.8	64	35	8/10	292.6	70.8	171.0	68.5	132.8	4.8	Sandstone

n and *N* are number of specimen measured and used for calculation, respectively. A mean direction is calculated at the reference point of Bikin (46.5°N, 134.7°E). Dec. and Inc. are declination and inclination respectively; k and α_{95} are the estimate of the Fisherian precision parameter and the radii of cone of 95 per cent confidence (Fisher 1953). Strikes of bedding are values before the subtraction of local geomagnetic declination (Mandea & Macmillan 2000).

10^{-2} A m^{-1}. Thermal treatment clearly revealed a single component of magnetization (Fig. 5). All the sites yielded very consistent unblocking temperatures pattern, where more than 95 per cent of the NRM intensity is removed between 300°C and 350°C (Figs 5a–c). *Insitu* site-mean direction for magnetic component with maximum unblocking temperatures of 350°C of four sites (BK10, BK11, BK12 and BK13) is $D = 249.1°$, $I = 64.1°$ ($\alpha_{95} = 11.2°$) (Fig. 5). After tilt correction, the dispersion of directions increases. The ratio of the precision parameter decreases after tilt correction ($k2/k1 = 8.1/68.4$). The optimal concentration of DC tilt test (Enkin 2003) is achieved at -18 ± 39 per cent. The McFadden's fold test (McFadden 1990) also shows negative results at 99 per cent confidence level, where the calculated value (ξ_1) is 2.319 in geographic coordinates and 3.829 after tilt correction, while the critical value (ξ) is 3.180 at 99 per cent confidence level. These behaviours very clearly indicate that this component magnetization in the sandstone of the Kultukha Formation was acquired after tilting as a secondary magnetization.

The secondary magnetization is observed in remanent magnetization remained up to the heating level of 500°C in BK13 (Fig. 5d and Table 1).

5 ROCK MAGNETISM

Thermal demagnetization of three-component IRMs (Lowrie 1990) was conducted on samples from all sites to elucidate the carrier of remanent magnetization (Fig. 6). The carrier of magnetization in the Albian welded tuffs and tuffs is magnetite, because the maximum unblocking temperatures of 560–590°C is obtained from thermal treatment of the NRM and three-component IRMs (Figs 3 and 6).

Based on the maximum unblocking temperature of about 330°C shown in thermal demagnetization of the NRM (Fig. 5), pyrrhotite is considered as main magnetic carrier in the Berriaisan sandstones. The presence of pyrrhotite is well defined by thermal treatment of the three-component IRMs, where the medium coercivity fraction sharply drops at 330°C (Fig. 6). Optical microscopic observation under transmitted and reflected light shows that the Berriaisan sandstones are low-grade metasedimentary rocks in which formation of metamorphic biotite takes plate. Fine-grained iron sulphides are abundant in three thin sections (BK10-1, BK11-3, BK12-8) from the sandstones of sites BK10, BK11 and BK12, but grain size is too small (less than a few μm) to identify pyrrhotite.

6 DISCUSSION

The ChRM isolated from the Albian welded tuffs of the Bikin area passes both the fold tests (McFadden 1990; Enkin 2003). The ChRM is not pyrrhotite but magnetite, and the upper Jurassic–Lower Cretaceous sedimentary layers in the Sikhote Alin orogenic belt were deformed prior to the Senonian (Zonenshain *et al.* 1990; Kirillova & Kiriyanova 2003). These facts favour the interpretation that the ChRM is a primary remanence. A tilt-corrected mean direction of this ChRM gives the ChRM direction of the Albian Alchanskaya Formation ($D = 309.3°$, $I = 68.7°$, $\alpha_{95} = 10.1°$, $N = 6$) with a corresponding pole position of 57.0°N, 76.8°E, $A_{95} = 12.4°$ (Table 1).

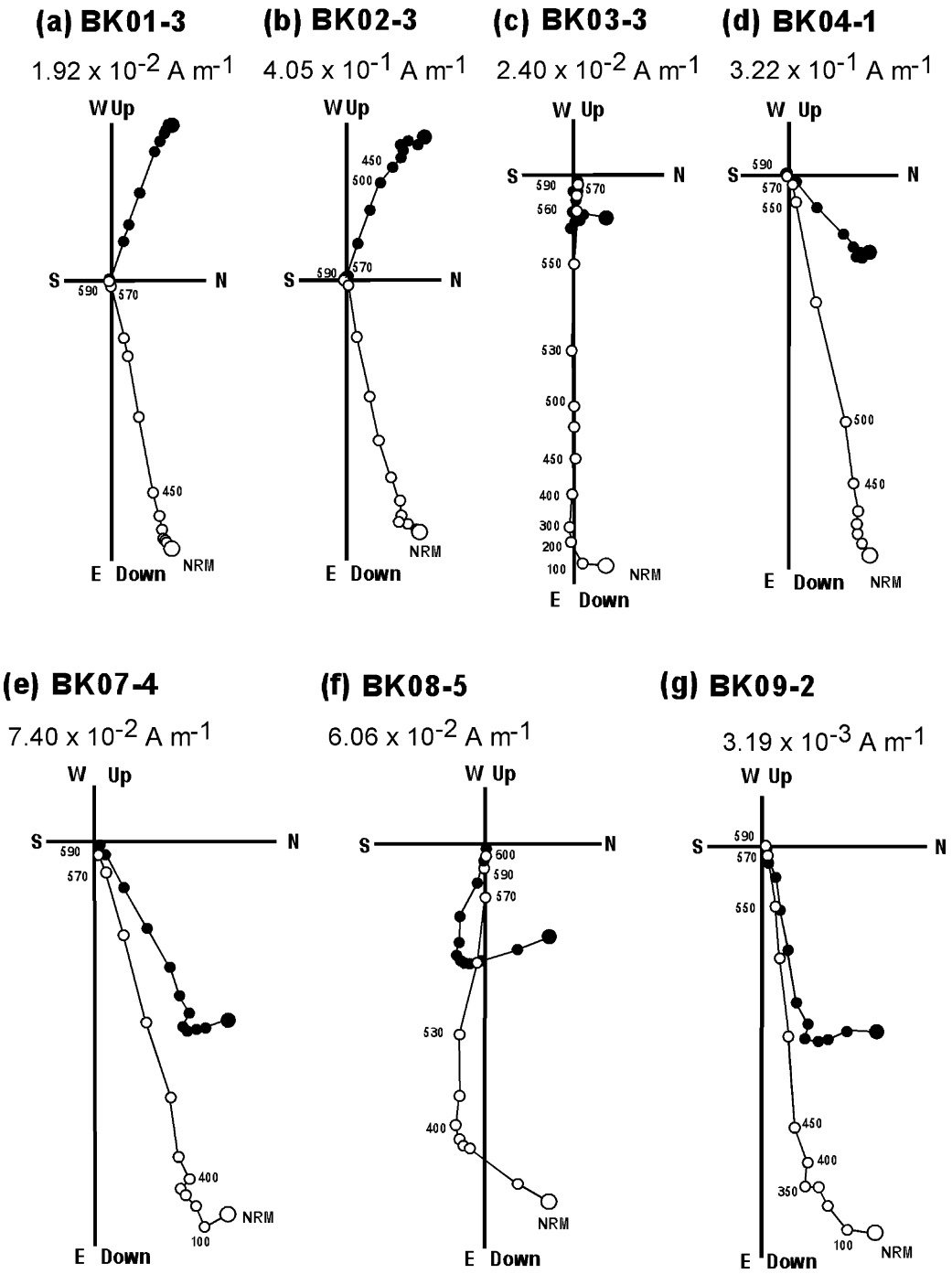

Figure 3. Zijderveld diagrams of the magnetization vector response to thermal demagnetization procedure for the Alchanskaya Formation. Numbers adjacent to demagnetization path are temperature in degree Celsius. (a, b, c, d, f, g) Samples from welded tuffs. (e) Samples from dacite tuffs. Open (solid) symbols show projection onto the vertical (horizontal) plane. All directions are plotted in geographic coordinates.

Although the ChRM of the Albian Alchanskaya Formation record just a spot reading of the ambient geomagnetic field, the west-directed direction most probably represents a record of the geomagnetic field for a fairly long period of time during Early Cretaceous. This statement is strongly supported by the following arguments. Firstly, the west-directed direction is recorded in the tuffs (site BK3) as well as in the welded tuffs, although longer geomagnetic field record is preserved in tuffs with DRM or PDRM, rather than in welded tuffs with TRM. Secondly, secondary magnetizations carried by pyrrhotite in the Berriasian Kultukha Formation are of west-directed declination. Because the Hauterivian to Cenomanian tectonic activity initiated formation of a metamorphic layer in the Sikhote Alin orogenic belt (Khanchuk 2001), this activity is presumably responsible for the secondary magnetizations associated with weak metamorphism. Combining the timing of folding, the west-directed direction of the Kultukha Formation is a record between Hauterivian and Early Late Cretaceous.

The west-directed declination ($D = 309.3^\circ$) obtained from the Bikin area is ascribable to tectonic rotation. The similar west-directed directions are observed at Qitaihe (Uchimura *et al.* 1996)

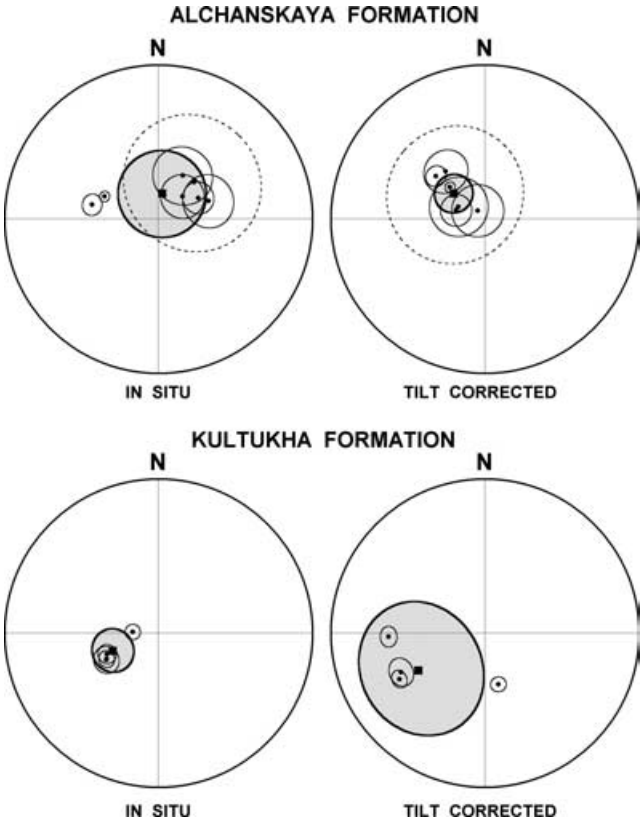

Figure 4. Equal-area projections of the site-mean directions with 95 per cent confidence circles for Alchanskaya and Kultukha Formation rocks. Alchanskaya Formation: Solid circles with 95 per cent confidence circles and a diamond with dotted 95 per cent confidence circle are data of dacite welded tuffs and dacite tuffs, respectively. Square with shaded circle of confidence indicates the mean direction based on the data of six sites of dacite welded tuffs. Kultukha Formation: solid circles with 95 per cent confidence circles are data for magnetization component with maximum unblocking temperature of 350°C. Square with shaded circle of confidence indicates the overall mean direction. All the symbols are for the lower hemisphere.

and Sikhote Alin (Uno *et al.* 1999; Otofuji *et al.* 2003) in the eastern part of Mongolia block (Figs 1 and 7). Palaeomagnetic study of the Late Jurassic to Early Cretaceous sedimentary rocks covers 30 × 70 km at the Qitaihe area in Heilongjiang province of China and palaeomagnetic sampling sites of the Late Cretaceous welded tuffs in Sikhote Alin study area are geographically distributed in 300 km range along the coast of Sikhote Alin volcanic belt of eastern Russia. Fig 7 shows pole positions for Bikin (57.0°N, 76.8°E, $A_{95} = 15.1°$), Qitaihe (61.9°N, 74.7°E, $A_{95} = 9.0°$) and Sikhote Alin (71.5°N, 38.9°E, $A_{95} = 9.9°$). They are plotted on the west side of the 100 Ma pole of Eurasia (Besse & Courtillot 1991) with respect to the eastern part of Mongolia block (Fig. 7). The west-directed directions in rocks with different ages from fairly large areas are not explained by any geomagnetic field behaviour (secular variation or excursion). We claim that the eastern part of the Mongolia block underwent CCW tectonic rotation with respect to Eurasia. Our new data showing the west-directed declinations from Bikin (46.5°N, 134.7°E) widely broadens the extent of region which experienced the large CCW rotation.

The CCW rotation of three areas (Bikin, Qitaihe and Sikhote Alin) in the eastern part of the Mongolia block is characterized by the large magnitude more than 36° with respect to the ambient regions. Comparison with the 100 Ma Eurasian pole indicates that the Bikin area was subjected to CCW rotation of 69.7° ± 29.9° without south–north translation (−0.9° ± 17.0°) with respect to Eurasia. Magnitudes of CCW rotation calculated for Qitaihe and Sikhote Alin volcanic belt are 39.2° ± 17.1° and 43.4° ± 16.6° with respect to Eurasia, respectively (Uchimura *et al.* 1996; Otofuji *et al.* 2003). Based on the combined Cretaceous reference pole for Mongolia and NCB by Lin *et al.* (2003), a CCW rotation of more than 35.7° ± 16.7° is expected for these areas with respect to Mongolia and NCB (Table 2).

The large CCW motion of the broad region requires a large-scale rotation model instead of the local rotation models in which the CCW motion of the Qitaihe and the southern part of Sikhote Alin was explained by either a ball bearing or bookshelf-type models due to the sinistral displacement along faults (Uchimura *et al.* 1996; Uno *et al.* 1999). The Qitaihe area is close to the northeastern extension of the Tan-Lu fault (Fushun Mishan Fault) and a sinistral displacement probably occurred during Jurassic–Cretaceous times (Xu & Zhu 1994; Zhang *et al.* 2003). The Sikhote Alin is assumed to be transformed into a rectangular block by the Central Sihote Alin fault and its branches (Uno *et al.* 1999). However, because Bikin area is far away from either northeastern extension of the Tan-Lu fault or the Central Sikhote Alin fault, the CCW rotation is hardly explained by the localized movement due to strike-slip faults.

Timing of this CCW rotation is an important clue to make a large-scale tectonic model for this region. Previous palaeomagnetic data from the Sikhote Alin area show that the Upper Campanian Kisin Group (Monastriskaya Suite) records a CCW rotation whereas no significant rotation (8.5° ± 17.0°) is detected from the Early Tertiary Bogopol Group (Otofuji *et al.* 1995, 2003). These data, thus, suggest that the most probable cause for rotational motion in this region (including Bikin, Sikhote Alin and Qitaihe areas) is ascribed to deformation during the Late Cretaceous to Palaeocene. The CCW rotational motion is contemporaneous with the post-Late Mesozoic tectonic phenomena of development of the Basin and Range type fault-basin systems in the eastern margin of the Aisan continent (Ren *et al.* 2002; Tian *et al.* 1992). The Middle Amur, Sanjian, Razdolnian, Amur-Zeya and Songliao basins distributed in the eastern part of the Mongolia block formed later than Santonian to Campanian (Kirillova 1995; Lin *et al.* 2003). Shape of the Middle Amur-Sanjian and Amur-Zeya basins is characterized by the Δ. Formation of these basins with isosceles triangle shape resulted in rotation of the Bikin, Sikhote Alin and Qitaihe areas in the eastern part of the Mongolia block.

The Mesozoic–Cenozoic rifting in the northeastern Chinese Plain, on the other hand, activated clockwise (CW) rotation in the northern part of the NCB (Fig. 1). Cretaceous palaeomagnetic direction reported from East Liaoning–Korean block shows an east-directed declination. Declination values from Kyongsang basin of the South Korea range between 28° and 37° (Otofuji *et al.* 1986; Lee *et al.* 1987; Zhao *et al.* 1999). Late Cretaceous declination values of 40.7° and 40.1° were reported from Upper Cretaceous rocks in the Benxi area of the Liaonign province (China) (Uchimura *et al.* 1996; Lin *et al.* 2003). Lin *et al.* (2003) estimated that the East Liaoning–Korean block experienced a CW rotation of 22.5° ± 10.2° with respect to the Chinese block (NCB + SCB). This CW rotation is ascribed to Late Cretaceous extension of the Xialiaohe and Songliao (Lin *et al.* 2003). Although formation of the Songliao basin continued from the Late Jurassic to the Neogene, a broad depression associated with second rifting phase developed during the Late Cretaceous (Ren *et al.* 2002). The Late Cretaceous rifting in the plains of northeast China played an important role in tectonic rotation of

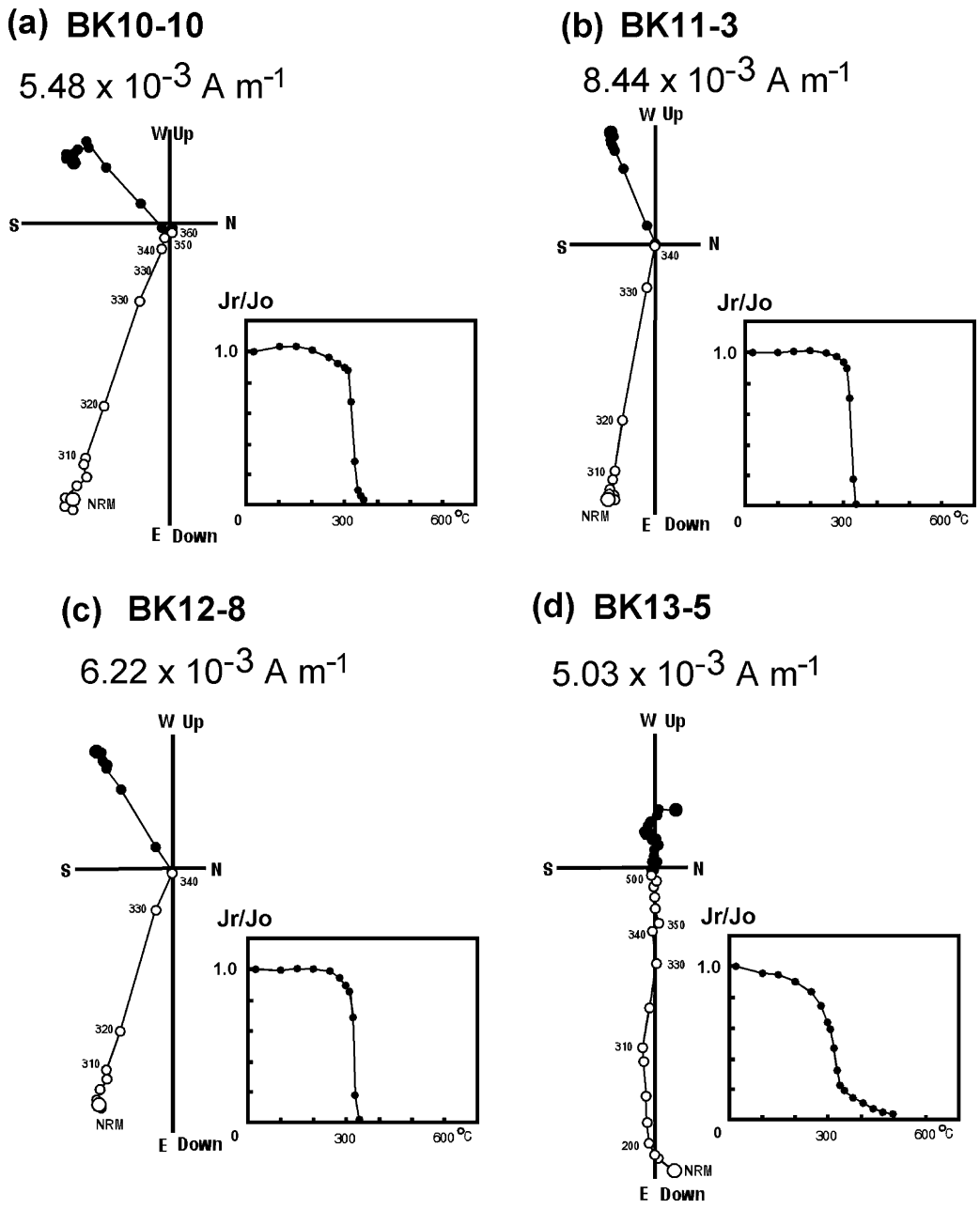

Figure 5. Zijderveld diagrams of the magnetization vector response to thermal demagnetization procedure for the Kultukha Formation, together with magnetic intensity decay curves. Numbers adjacent to demagnetization path in Zijderveld diagrams are temperature in degree Celsius. Abrupt decreases of remanent intensity is very clearly indicated between 300°C and 350°C in all specimens, suggesting the presence of pyrrhotite. All directions are plotted in geographic coordinates.

the East Liaoning–Korean block as well as the eastern margin of the Mongolia block.

The available palaeomagnetic data show sequential opposite tectonic rotations of blocks along the eastern margin of the Asian continent later than Cretaceous. The Late Cretaceous to Palaeocene phenomena is that the CCW rotation for eastern margin of the Mongolia block and the CW rotation for eastern margin of the NCB. Early Miocene opposite tectonic rotations is the double door opening mode of the Japan Sea associated with differential motion of the Japanese islands (Otofuji *et al.* 1985). These tectonic features imply that the eastern margin of the Asian continent encountered same type of tectonic phenomenon during both the Late Cretaceous and the Miocene. However, such phenomena are hardly ascribed to lateral extrusion of the East Asia due to India–Asia collision (Fournier *et al.* 2004), because India collided to Asia once around 55 Ma (Rowley 1996) after the opposite rotations in the eastern margin of the Mongolia block.

Sequentially occurred opposite tectonic rotations of blocks are associated with opening of basins along the eastern margin of the Asian continent, suggesting that extensional regime repeatedly operated after the Late Cretaceous (Fig. 8). Geophysical observations from the Songliao basin suggest that the Late Cretaceous rifting phase was accompanied by lithosphere stretching, crustal thinning and mantle upwelling (Ma 1987; Hsu 1989). For the Miocene

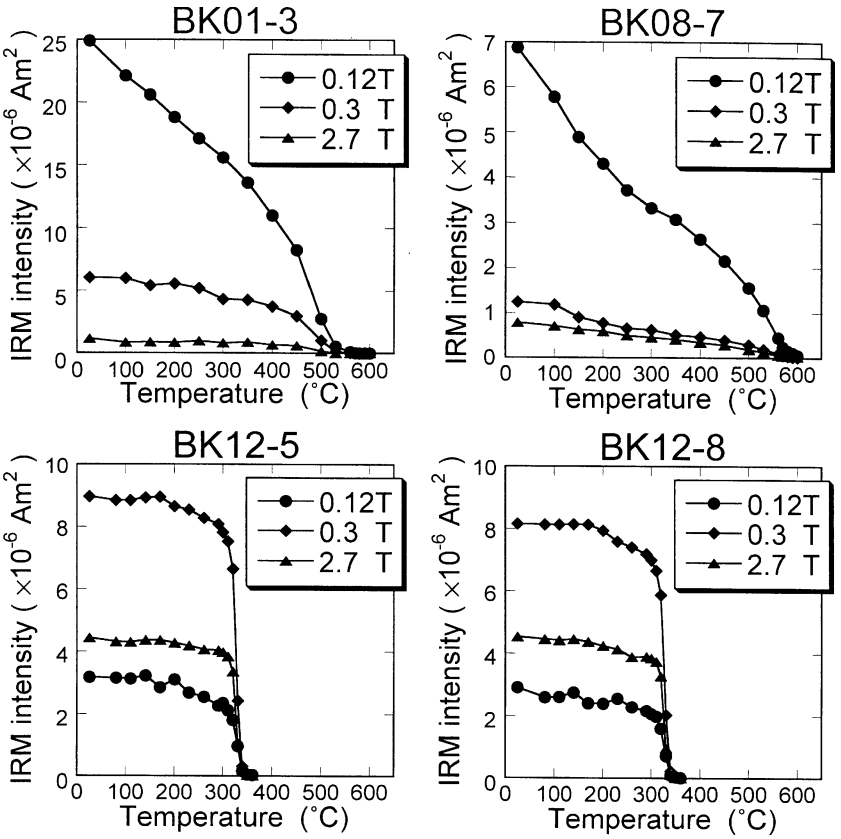

Figure 6. Thermal demagnetization of three-component IRMs for (a, b) welded tuffs of the Alchanskaya Formation and (c, d) sandstones of the Kultukha Formation. IRMs of different DC fields (2.7 T, 0.3 T, 0.12 T) were imparted to three perpendicular axes of the specimen and then thermally demagnetized. The unblocking temperature for pyroclastic specimens (BK01-3 and BK08-7) is between 500°C and 580°C, whereas for sandstone specimens (BK12-5 and BK12-8) it is around 350 °C.

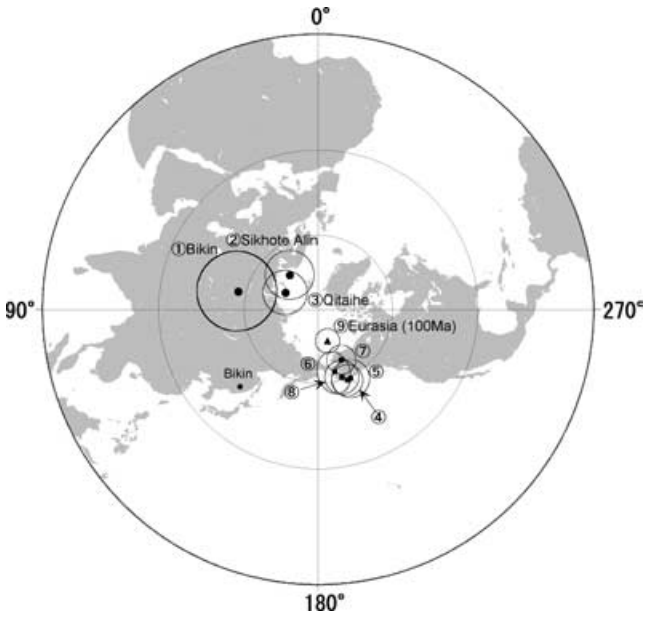

Figure 7. Palaeomagnetic poles with associated circles of 95 per cent confidence level for eastern Mongolia are shown by circles (Bikin, Sikhote Ain and Qitaihe). Poles for the NCB are shown by squares (two poles from Benxi and three from Kyongsang basin). The 100 Ma reference pole for Eurasia (Besse & Courtillot 1991) is marked by triangle. The numbers adjacent to poles represent the corresponding localities in Table 2.

opening of the Japan Sea, mass upwelling of asthenosphere and/or eastward flow of asthenosphere has been suggested (Tatsumi *et al.* 1989; Nohda *et al.* 1988; Okamura *et al.* 2005). Periodic extension can be explained by 2-D mantle convection, which has intermittently occurred along a continental margin. Numerical models in which a supercontinent covers a top surface of a convection layer induce lateral and sequential mantle flows toward the ocean associated with periodic plume generation (Gurnis 1988; Lowman & Jarvis 1996; Honda *et al.* 2000). Episodic backarc extension took place in the western–central Mediterranean basins (Carminati *et al.* 1998), which is ascribed to slab detachment process (Carminati *et al.* 1998; Faccenna *et al.* 2001). It is possible that repeated occurred lateral mantle flow, toward the ocean, in combination with the dynamic evolution of the subducting oceanic lithosphere is one of the most important factors for the periodic extension of East Asian basins.

7 CONCLUSION

Previous and the newly presented palaeomagnetic data show that a fairly broad area along the eastern margin of the Mongolia block experienced CCW rotation. CCW rotation was most likely responsible for Late Cretaceous extension along the northeast Chinese basins (e.g. Middle Amur, Sanjian, Razdolnian, Amur-Zeya and Songliao basins). Comparing with CW rotation of the eastern margin of the East Liaoning–Korean block, opposite tectonic rotations took place along the eastern margin of the Asian continent. This opposite tectonic rotations for fairly wide-ranging areas is associated with fan

Table 2. Cretaceous palaeomagnetic results from eastern margin of the Mongolia block and the NCB.

Locality name	Lat.(°N)	Long.(°E)	Age	Observed direction N	Dec.(°)	Inc.(°)	α_{95}(°)	Pole Position Lat.(°N)	Long.(°E)	A_{95}(°)	Rotation R(°)	Reference
Eastern margin of the Mongolia block												
(1) Bikin	46.5	134.7	K1	6	309.3	68.7	10.1	57.0	76.8	12.4	-69.7 ± 29.9	this study
(2) Sikhote Alin	44.0	135.0	K2	35	335.6	54.4	8.5	71.5	38.9	9.9	-43.4 ± 16.6	Uno *et al.* (1999), Otofuji *et al.* (2003)
(3) Qitaihe	45.8	131.0	J3-K1	20	338.8	65.6	6.2	74.7	61.9	9.0	-39.2 ± 17.1	Uchimura *et al.* (1996)
Eastern margin of the NCB												
(4) Benxi	41.3	123.8	K2	5	40.7	59.0	4.7	59.3	202.6	6.0	22.9 ± 11.5	Uchimura *et al.* (1996)
(5) Bemxi	41.3	123.8	K2	7	40.1	57.9	7.3	59.4	205.5	7.3	22.3 ± 15.4	Lin *et al.* (2003)
(7) Kyongsang basin	36.0	128.5	K	60	33.0	60.9	5.5	64.0	195.0	6.4/8.4	16.8 ± 13.1	Otofuji *et al.* (1986)
(8) Kyongsang basin	36.0	129.0	K1	19	28.1	57.5	5.0	67.6	205.1	5.8	11.9 ± 11.4	Lee *et al.* (1987)
(9) Kyongsang basin	36.0	129.0	K1	9	37.4	57.9	6.6	61.2	199.5	6.6	21.2 ± 14.1	Zhao *et al.* (1999)
Creatceous Reference Poles												
(9) Eurasia			100 Ma					76.7	197.1	5.0		Besse & Courtillot (1991)
(10) Mongolia and NCB			K	8				79.8	200.6	4.5		Lin *et al.* (2003)

J3: Late Jurassic, K: Cretaceous; K1: Early Cretaceous, K2: Late Cretaceous. N: number of localities used for the calculation of palaeomagnetic direction or pole, Dec. and Inc.: declination and inclination, respectively; $\alpha_{95:}$ and A_{95}: the radius of the cone of 95 per cent confidence. Lat. and Long.: latitude and longitude, respectively. R: magnitude of rotation with respect to Eurasia and its uncertainty of 95 per cent confidence after Butler (1992).

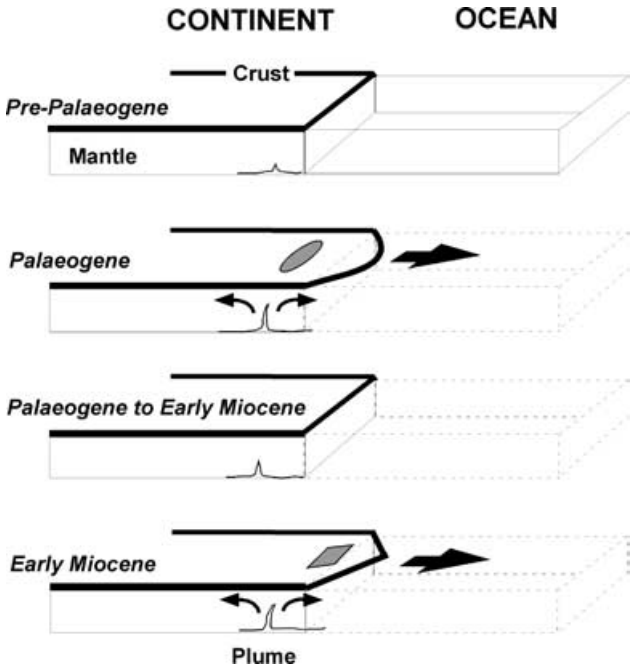

Figure 8. A periodic extension model. Periodic extension (black arrow) on a continental margin can be explained by 2-D mantle convection, which has intermittently occurred along the continental margin. These extensions result in opening of basins (grey areas) in the outer margin of the continent and sometimes lead to continental fragment breaking away from the mother continent. The northeast Chinese basins (e.g. Middle Amur, Sanjian, Razdolnian, Amur-Zeya and Songliao basins) and Japan Sea opened at Cretaceou–Palaeogene and Early Miocene times in the eastern margin of the Asian continent, respectively. Continental margin outside of the basins experienced opposite rotation associated with basin formation. Induction of small-scale convection associated with periodic plume generation is after a model by Lowman & Jarvis (1996) in which the supercontinent covers a top surface of a convection layer.

shaped opening of basins in the northeast Chinese Plain later than the Late Cretaceous. Late Cretaceous opening of the continental basins was followed by the double door opening of the Japan Sea along the East Asian margin in Miocene (Otofuji *et al.* 1985).

ACKNOWLEDGMENTS

The efficient field logistics were set up by the Pacific Oceanological Institute (POI). We are indebted to Tetsumaru Itaya for discussion on microscopic observation. We thank Drs. E. Appel, J. W. Geissman and R.J. Enkin for their critical reviews on the manuscript. This work was supported in part by the Toyota Foundation, the Hyogo Science and Technology Association, and Grant-in-aid (No. 14403010) from Japanese Ministry of Education, Culture, Sports, Science and Technology (MEXT) and 'The 21st Century COE Program of Origin and Evolution of Planetary Systems' in MEXT (Japan).

REFERENCES

Besse, J. & Courtillot, V., 1991. Revised and synthetic apparent polar wander paths of the African, Eurasian, North American and Indian plates, and true polar wander since 200 Ma, *J. geophys. Res.,* **96,** 4029–4050.

Butler, R.F., 1992. *Paleomagnetism*, 319pp, Blackwell Scientific Publications, Boston, Massachusetts.

Carminati, E., Wortel, M.J.R., Spakman, W. & Sabadini, R., 1998a. The role of slab detachment processes in the opening of the western-central Mediterranean basins: some geological and geophysical evidence, *Earth planet. Sci. Lett.,* **160,** 651–665.

Carminati, E., Wortel, M.J.R., Spakman, W. & Sabadini, R., 1998b. The two-stage opening of the western-central Mediterranean basins: a forward modeling test of a new evolutionary model, *Earth planet. Sci. Lett.,* **160,** 667–679.

Enkin, R.J., 2003. The direction-correction tilt test: an all-purpose tilt/fold test for paleomagnetic studies, *Earth planet. Sci. Lett.,* **212,** 151–166.

Faccenna, C., Funiciello, F., Giardini, D. & Lucente, P., 2001. Episodic back-arc extension during restricted mantle convection in the central Mediterranean, *Earth planet. Sci. Lett.,* **187,** 105–116.

Fisher, R.A., 1953. Dispersion on a sphere, *Proc. R. Soc. London, Ser. A,* **217,** 295–305.

Flower, M.F.J., Russo, R.M., Tamaki, K. & Hoang, N., 2001. Mantle contamination and the Izu-Bonin-Mariana (IBM) 'high-tide mark': evidence for mantle extrusion caused by Tethyan closure, *Tectonophysics,* **333,** 9–34.

Fournier, M., Jolivet, L., Davy, P. & Thomas, J-C., 2004. Backarc extension and collision: an experimental approach to the tectonics of Asia, *Geophys. J. Int.,* **157,** 871–889.

Gurnis, M., 1988. Large-scale mantle convection and the aggregation and dispersal supercontinents, *Nature,* **332,** 695–699.

Honda, S., Yoshida, M., Ootorii, S. & Iwase, Y., 2000. The timescales of plume generation caused by continental aggregation, *Earth planet. Sci. Lett.,* **176,** 31–43.

Hsu, K.J., 1989. Origin of sedimentary basins of China. Chinese sedimentary basins, in *Sedimentary Basins of the World*, pp. 207–227, ed. Zhu, X., Elsevier, Amsterdam.

Khanchuk, A.I., 2001. Pre-Neogene tectonics of the Sea-of-Japan region: a view from the Russian side, *Earth Science,* **55,** 275–291.

Kirillova, G.L. & Kiriyanova, V., 2003. J/K boundary in southeastern Russia and possible analogue of the Tetori Group, Japan, *Memoir of the Fukui Prefectural Dinosaur Museum,* **2,** 75–102.

Kirillova, G.L., 1995. Late Mesozoic environmental history of south-eastern Russia, IGCP project 350, in *Environmental and tectonic history of East and South Asia*, pp. 93–107, Proc. of 15th International Symposium of Kyungpook National University.

Kirschvink, J.L., 1980. The least-squares line and plane and the analysis of palaeomagneitc data, *Geophys. J. R. astr. Soc.,* **62,** 699–718.

Kravchinsky, V.A., Sorokin, A.A. & Courtillot, V., 2002. Paleomagentism of Paleozoic and Mesozoic sediments from the southern margin of Mongol-Okhotsk ocean, far eastern Russia, *J. geophys. Res.,* **107**(B10), 2253, doi:10.1029/2001JB000672.

Lee, G., Besse, J. & Courtillot, V., 1987. Eastern Asia in the Cretaceous: New paleomagnetic data from South Korea and a new look at Chinese and Japanese data, *J. geophys. Res.,* **92,** 3580–3596.

Li, Z.X., 1998. Tectonic history of the Major East Asian Lithospheric Blocks since the Mid-Proterozoic—a synthesis, in *Mantle Dynamics and Plate Interactions in East Asia*, pp. 221–243, eds Flower, M.F.J., Chung, S-L., Lo, C-H. & Lee, T-Y., Geodynamics Series 27, AGU, Washington DC.

Lin, W., Chen, Y., Faure, M. & Wang, Q., 2003. Tectonic implications of new Late Cretaceous paleomagnetic constraints from Eastern Liaoning Peninsula, NE China, *J. geophys. Res.,* **108**(B6), 2305, doi:10.1029/2002JB002169.

Lowman, L.P. & Jarvis, G.T., 1996. Continental collisions in wide aspect ratio and high Rayleigh number two-dimensional mantle convection models, *J. geophys. Res.,* **101,** 25 485–25 497.

Lowrie, W., 1990. Identification of ferromagnetic minerals in a rock by coercivity and unblocking temperature properties, *Geophys. Res. Lett.,* **17,** 159–162.

Ma, X.Y., 1987. *Lithospheric dynamics map of China and adjacent seas (1:4,000,000) and exploratory notes (in Chinese),* map, Geol. Publ. House, Beijing.

Mandea, M. & Macmillan, S., 2000. International geomagnetic reference field-the eighth generation, *Earth Planets Space,* **52,** 1119–1124.

McFadden, P.L., 1990. A new fold test for palaeomagnetic studies, *Geophys. J. Int.,* **103,** 163–169.

Meng, Q.-R., 2003. What drove late Mesozoic extension of the northern China-Mongolia tract?, *Tectonophysics,* **369,** 155–174.

Natal'in, B., 1993. History and modes of Mesozoic accretion in Southeastern Russia, *The Island arc,* **2,** 15–34.

Nohda, S., Tatsumi, Y., Otofuji, Y., Matsuda, T. & Ishizaka, K., 1988. Asthenospheric injection and back-arc opening: Isotopic evidence from Northeast Japan, *Chem. Geol.,* **68,** 317–327.

Northrup, C.J., Royden, L.H. & Burchfiel, B.C., 1995. Motion of the Pacific plate relative to Eurasia and its potential relation to Cenozoic extension along the eastern margin of Eurasia, *Geology,* **23,** 719–722.

Okamura, S., Arculus, R.J. & Maretynov, Y.A., 2005. Ceozoic magnetism of the north-eastern Eurasian margin: the role of lithosphere versus asthenospher, *J. Petrol.,* **46,** 221–253.

Otofuji, Y., Matsuda, T. & Nohda, S., 1985. Opening mode of the Japan Sea inferred from the palaeomagnetism of the Japan Arc, *Nature,* **317,** 603–604.

Otofuji, Y., Kim, K.H., Inokuchi, H., Morinaga, H., Murata, F., Katao, H. & Yaskawa, K., 1986. A paleomagnetic reconnaissance of Permian to Cretaceous sedimentary rocks in southern part of Korean Peninsula, *J. Geomag. Geoelectr.,* **38,** 387–402.

Otofuji, Y. *et al.*, 1995. Late Cretaceous to early Paleogene paleomagnetic results from Sikhote Alin, far Eastern Russia: implications for deformation of East Asia, *Earth Planet. Sci. Lett.,* **130,** 95–108.

Otofuji, Y. *et al.*, 2002. Internal deformation of Sikhote Alin volcanic belt, far eastern Russia: Paleocene paleomagnetic results, *Tectonophysics,* **350,** 181–192.

Otofuji, Y. *et al.*, 2003. Late Cretaceous palaeomagnetic results from Sikhote Alin, far eastern Russia: tectonic implications for the eastern margin of the Mongolia block, *Geophys. J. Int.,* **152,** 202–214.

Ren, J., Tamaki, K., Li, S. & Junxia, Z., 2002. Late Mesozoic and Cenozoic rifting and its dynamic setting in Eastern China and adjacent areas, *Tectonophysics,* **344,** 175–205.

Rowley, D.B., 1996. Age of initiation of collision between India and Asia: A review of stratigraphic data, *Earth planet. Sci. Lett.,* **145,** 1–13.

Tatsumi, Y., Otofuji, Y., Matsuda, T. & Nohda, S., 1989. Opening of the sea of Japan back-arc basin by asthenospheric injection, *Tectonophysics,* **166,** 317–329.

Tian, Z.Y., Han, P. & Xu, K.D., 1992. The Mesozoic-Cenozoic East China rift system, *Tectonophysics,* **208,** 341–363.

Uchimura, H., Kono, M., Tsunakawa, H., Kimura, G., Wei, Q., Hao, T. & Liu, H., 1996. Paleomagnetism of late Mesozoic rocks from northeastern China: the role of the Tan-Lu fault in the North China Block, *Tectonophysics,* **262,** 301–319.

Uno, K. *et al.*, 1999. Late Cretaceous paleomagnetic results from Northeast Asian continental margin: the Sikhote Alin mountain range, eastern Russia, *Geophys. Res. Lett.,* **26,** 553–556.

Uyeda, S. & Kanamori, H., 1979. Back-arc opening and the mode of subduction, *J. geophys. Res.,* **84,** 1049–1061.

Xu, J. & Zhu, G., 1994. Tectonic models of the Tan-Lu fault zone, Eastern China, *Int. Geo. Rev.,* **36,** 771–784.

Yokoyama, M., Liu, Y., Halim, N. & Otofuji, Y., 2001. Paleomagnetic study of Upper Jurassic rocks from the Sichuan basin: tectonics aspects for the collision between the Yangtze block and the North China Block, *Earth planet. Sci. Lett.,* **193,** 273–285.

Zhang, Y., Dong, S. & Shi, W., 2003. Cretaceous deformation history of the middle Tan-Lu fault zone in Shandong Province, eastern China, *Tectonophysics,* **363,** 243–258.

Zhao, X. & Coe, R.S., 1987. Palaeomagnetic constraints on the collision and rotation of North and South China, *Nature,* **327,** 141–144.

Zhao, X.X. *et al.*, 1999. Clockwise rotations recorded in Early Cretaceous rocks of South Korea: implications for tectonic affinity between the Korean Peninsula and North China, *Geophys. J. Int.,* **139,** 447–463.

Zijderveld, J.D.A., 1967. A.C. demagnetization of rocks: Analysis of results, in *Methods in Palaeomagnetism*, pp. 254–286, eds Collinson, D.W., Creer, K.M. & Runcorn, S.K., Elsevier, Amsterdam.

Zonenshain, L.P., Kuzmin, M.I. & Natapov, L.M., 1990. Geology of the USSR: a plate-tectonic synthesis, *Geodyn. Ser.,* Vol. 21, p. 242, ed. B.M. Page, AGU, Washington DC.